copurified mixture of isoforms using methods adapted from S. S. Tang, P. C. Trackman, and H. M. Kagan [*J. Biol. Chem.* **258**, 4331 (1983)]. The enzyme was measured in 4*M* urea extracts of skin samples [H. M. Kagan and K. A. Sullivan, *Methods Enzymol.* **82A**, 637 (1982)] by an enzyme-linked immunoassay. The net accumulation of lysyl oxidase in the extracellular matrix of dorsal skin (in micrograms per gram ± SEM) was reduced from 500 ± 123 to 146 ± 55 by week 8 ($P < 0.01$; for two replicates, $n = 4$ to 6 each). The lysyl oxidase antibody preparation and the enzyme-linked immunoassay were done as described by H. Bode and H. Stegeman [*J. Immunol. Methods* **72**, 421 (1984)] and S. B. Carroll and B. D. Stallar [*J. Biol. Chem.* **258**, 24 (1983)]. A preliminary report on the characterization of lysyl oxidase and its quantitation by enzyme-linked immunosorbent assay (ELISA) has been published by D. Tinker, N. Romero, and R. B. Rucker [*FASEB J.* **3**, 624A (1989)].

9. C. G. Kindberg and J. W. Suttie, *J. Nutr.* **119**, 175 (1989); D. Balnave, *Am. J. Clin. Nutr.* **30**, 1408 (1977).
10. J. R. Pleasants, M. H. Johnson, B. S. Wostmann, *J. Nutr.* **116**, 1949 (1986); W. R. Farkas, *J. Biol. Chem.* **255**, 6832 (1980); R. L. Walzem and A. J. Clifford, *J. Nutr.* **118**, 1089 (1988).
11. H. M. Hanauske-Abel, G. Tschank, V. Günzler, E. Baader, P. Gallop, *FEBS Lett.* **214**, 236 (1987).
12. M. Ameyama *et al.*, *BioFactors* **1**, 51 (1988); M. Ameyama *et al.*, *Agric. Biol. Chem.* **49**, 699 (1985).

13. Supported by NIH grants HL-15965 and AM-35747 and a grant from the USDA. Care for animals was in accordance with NIH and USDA guidelines.

28 April 1989; accepted 11 July 1989

Translational Blockade Imposed by Cytokine-Derived UA-Rich Sequences

VÉRONIQUE KRUYS, OLIVIER MARINX, GRAY SHAW, JACQUELINE DESCHAMPS,* GEORGE HUEZ

The messenger RNAs specifying certain proteins involved in the inflammatory response and certain oncoproteins contain a conserved UA-rich sequence in the 3′ untranslated region. This sequence, which is composed of several interspersed repeats of the octanucleotide UUAUUUAU, has been shown to destabilize mRNA in some eukaryotes. However, this effect is not seen when mRNAs are transferred to *Xenopus* oocytes, which made it possible to separate stability from translational regulation. For interferon, granulocyte-macrophage colony-stimulating factor, and c-*fos* RNAs, the UA-rich sequence was observed to preclude mRNA translation.

THE MODULATION OF THE TRANSLATIONAL efficiency is an important post-transcriptional regulation of eukaryotic gene expression. Various characteristics of messenger RNAs are known to markedly influence translation efficiency. Several features present at the 5′ end of the molecule have been shown to be prerequisites for efficient translation of a eukaryotic mRNA: the presence of a cap structure (*1*), a favorable context surrounding the AUG initiation codon (*2*), the absence of stable secondary structures, and of an out-of-frame initiation codon (*3, 4*). At the 3′ end, the presence of polyadenylate [poly(A)] not only enhances mRNA stability (*5*) but also appears to affect the translation of some mRNAs (*1, 6*). Recently, the translational efficiency of several mRNAs has been shown to be specifically regulated by the presence of structural elements located in the 5′ or 3′ untranslated regions (UTRs) (*7, 8*). However, the mechanisms by which these post-transcriptional controls are specifically mediated are still not elucidated.

We have previously reported that the 3′ untranslated region of the human interferon-β (Hu–IFN-β) mRNA has an inhibitory effect on translation in certain systems like the reticulocyte lysate or the *Xenopus* oocytes. Furthermore, the addition of this Hu–IFN-β 3′ UTR at the 3′ end of the chicken lysozyme mRNA also leads to a large decrease of its translational capability in both systems (*9*). We have also shown that the poor translational efficiency of the Hu-IFN-β mRNA is not caused by a rapid degradation of the molecule. In contrast to what occurs in somatic cells, where this

V. Kruys, O. Marinx, G. Huez, Département de Biologie Moléculaire, Université Libre de Bruxelles, 67, rue des Chevaux, 1640 Rhode-Saint-Genèse, Belgium.
G. Shaw, Genetics Institute Incorporated, 87 Cambridge Park Drive, Cambridge, MA 02140.
J. Deschamps, Molecular Biology and Virology Laboratory, The Salk Institute, P.O. Box 85800, San Diego, CA 92138.

*Present address: Hubrecht Laboratory, Netherlands Institute for Developmental Biology, 8, Uppsalalaan, 3584 CT Utrecht, the Netherlands.

Fig. 1. The 3′ untranslated sequence of the different IFN-β mRNA constructs. The sequence is numbered from first nucleotide of the stop codon. The first 103 nucleotides of the sequence [bold letters symbolized by soIF (1–103)] are common to all constructs. In each modified construct, the natural last 99 nucleotides have been replaced by an oligonucleotide containing the UA sequence either in variable number (underlined) or modified (dotted underlined). All the SP6 plasmids encoding the Hu–IFN-β were constructed with the basic psoIF vector previously described (*11*). The in vitro transcribed IFN-β mRNA from this psoIF plasmid contains as 5′ UTR a short synthetic 19-nucleotide-long sequence. In DNA constructs psoIF $(UA)_1$, psoIF $(UA)_2$, psoIF $(UA)_3$, psoIF $(UA)_{AU}$, and psoIF $(UA)_{GC}$, the natural translation inhibitory sequence (62 nucleotides) was replaced by double-stranded oligodeoxynucleotides corresponding, respectively, to one, two, and three copies of the octanucleotide, or to one copy of a consensus sequence that is either modified or enriched in G and C residues. These oligodeoxynucleotides were inserted in the psoIF plasmid previously digested by Nde I and Xba I to remove the natural translation inhibitory sequence.

mRNA is short-lived (*10*), it remains remarkably stable in *Xenopus* oocytes even when not poly(A)$^+$. We have further identified a 62-nucleotide sequence in the IFN-β mRNA 3′ UTR that contains the structural feature responsible for the observed translation inhibition. This sequence is located between nucleotides 100 and 162 downstream from the termination codon and retains its inhibitory effect when moved to various positions downstream from the stop codon within long or short 3′ UTRs. On the other hand, it is no longer effective when inserted upstream from the AUG initiation codon (*11*). This 62-nucleotide-long segment is 85% UA-rich and contains several repeats of the consensus sequence UUAUUUAU. Similar UA-rich sequences also occur in the 3′ UTR of numerous lymphokine, cytokine, and protooncogene mRNAs (*12*) and have been shown to be the recognition signal for selective mRNA degradation (*13*).

To determine whether this UA-rich sequence is actually the translation-inhibitory element during translation in *Xenopus* oocytes, we synthesized an IFN-β mRNA where the last 100 nucleotides of the 3′ UTR were replaced by a series of three copies of the octanucleotide UUAUUUAU (Fig. 1). The translation efficiency of soIF $(UA)_3$ was much less than that of soIF/d 100–203, in which the translation inhibitory sequence was deleted. To examine whether the extent of the inhibition is related to the number of UA-rich octanucleotides present in the 3′ UTR, we synthesized two other constructs where the last 100 nucleotides were replaced by only one [soIF $(UA)_1$] or two [soIF $(UA)_2$] copies of the octanucleotide. Translation inhibition increased with the copy number of the octanucleotides present at the 3′ end of the mRNA (Fig. 2A). Two other mRNA constructs were synthesized next: in one of them, soIF $(UA)_{AU}$, the octanucleotide sequence was randomized and in the other, soIF $(UA)_{GC}$, the sequence was enriched in G and C residues (Fig. 1). The replacement of three A or U residues by G or C nucleotides abolished the translation inhibitory effect of the consensus sequence (Fig. 2B). The randomization of the sequence also lowered its

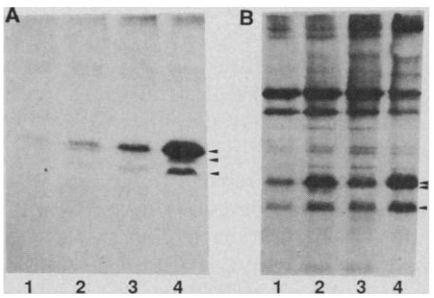

Fig. 2. Translation in *Xenopus* oocytes of the IFN-β mRNA constructs containing either an increasing number of UA-rich octanucleotides or a modified AU sequence. (**A**) Lane 1, soIF $(UA)_3$; lane 2, soIF $(UA)_2$; lane 3, soIF $(UA)_1$; and lane 4, soIF/d 100–203. (**B**) Lane 1, soIF $(UA)_1$; lane 2, soIF/d 100–203; lane 3, soIF $(UA)_{AU}$; and lane 4, soIF $(UA)_{GC}$. The three bands marked by arrowheads correspond to the different stages of glycosylation. Before transcription, the plasmids were linearized with the appropriate restriction enzymes: Nde I for psoIF/d 100–203, and Hind III for psoIF (UA), psoIF $(UA)_1$, psoIF $(UA)_2$, psoIF $(UA)_3$, psoIF $(UA)_{AU}$, and psoIF $(UA)_{GC}$. The injection procedure and the incubation of the oocytes have been described (*11*). After injection, the oocytes were incubated for 6 hours at 18°C in Barth's medium (0.01 ml per oocyte) containing ^{35}S-labeled methionine (9 μCi per oocyte) and 10% bovine serum albumin. The oocytes were lysed, and for each batch, ^{35}S-labeled oocyte extract (2.5 × 10^6 count/min) was immunoprecipitated with a goat polyclonal antibody to human IFN-β.

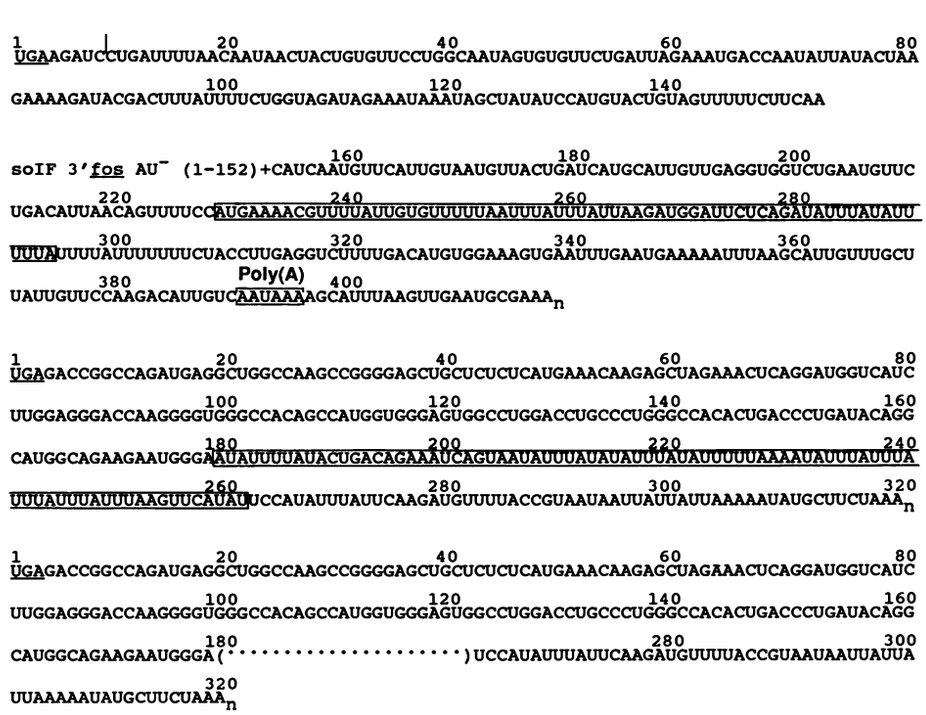

Fig. 3. The 3′ untranslated sequence of the (**A**) IFN-β–c-*fos* and (**B**) GM-CSF mRNAs. Both sequences are numbered from the first nucleotide of the stop codon. The boundary between the IFN-β and c-*fos* sequences of the chimeric IBN-β–c-*fos* is indicated by a short vertical line. The sequence in the solid box corresponds to the UA-rich region, the removal of which confers transforming activity to the mouse c-*fos* gene when appropriately expressed (*23*). In psoIF 3′ human *fos* AU$^-$, the sequences beyond nucleotide 152 are not present. This deletion as well confers transforming activity to human c-*fos* sequences (*24*). For the GM-CSF sequence, the solid box corresponds to the UA-rich region deleted in the SP64GMAU$^-$. The plasmids psoIF 3′*fos* and psoIF 3′*fos* AU$^-$ were constructed by inserting filled-in Pvu II–Eco RI 3′*fos* fragments in the psoIF vector previously digested with Bgl II and Bam HI and filled in with the Klenow polymerase. The 3′*fos* and 3′*fos* AU$^-$ fragments that were 406- or 144-bp-long, respectively, are derived from non–full-length cDNA clones isolated from a human placenta cDNA library (*24*). To construct pSP64GM and pSP64GMAU$^-$, site-directed mutagenesis was performed on plasmid pCSF-1 (*25*) by means of an oligonucleotide having the sequences: 5′-TTGAATAAATATGGATCCCATTCTTCTGCC-3′. The resulting plasmid pGM-CSF AU$^-$ had 83 bp deleted from the 3′ untranslated region of the GM-CSF cDNA. Plasmid pSP64 was digested with Eco RI and Pvu II, and the large fragment was purified and ligated with a pair of annealed oligonucleotides having the sequences: 5′-AATTC$(A)_{20}$GATCTCGAG-CAG-3′ and 5′-CTGCTCGAGATC$(T)_{20}$G-3′. The resulting plasmid, pSP64A20 was purified and restricted with Pst I and Eco RI, and the large fragment was ligated with the 750-bp Pst I–Eco RI fragment of pCSF or the ~677-bp fragment of pGMCSFAU$^-$. The resulting plasmids, p64GM or p64GMAU$^-$, were purified and restricted with Hind III, Pst I, and the large fragments were ligated with a pair of annealed oligonucleotides having sequence: 5′-AGCTTCTCGAGCCACCATGGCCTGCA-3′ and 5′-GGCC-ATGGTGGCTCGAGA-3′. The resulting plasmids were designated pSP64GM + ATG and pSP64FMAU$^-$ + ATG.

inhibitory effect relative to that observed with soIF $(UA)_1$, but did not inhibit it completely.

Altogether, these results show that one UA-rich consensus sequence constitutes a translation-inhibitory element. The clustering of A and U residues appears to be important since the inhibition is completely abolished when G and C residues are interspersed in the sequence. However, the exact order of the nucleotides seems to be less crucial than the UA content. This degree of flexibility in the sequence required may facilitate modulation of the extent of the translation inhibition. The level of translation inhibition also increased with the copy number of the UA-consensus sequence. With three copies, the translation of the IFN-β mRNA was inhibited to the same extent as with the natural UA-rich sequences. This may result from the fact that factors bind more efficiently to the 3′ untranslated region when several UA-consensus motifs are present (*14*).

We next examined whether the UA-rich sequences present in the 3′ UTR of other mRNAs also affect their translation. Therefore, we synthesized two different types of mRNAs: one, SP64GM, encoding the human granulocyte-macrophage colony-stimulating factor (GM-CSF), and the other, soIF 3′*fos*, coding for the IFN-β, but where the natural 3′ UTR was replaced by the last 406 nucleotides of the human c-*fos* mRNA 3′ UTR (Fig. 3). The translation efficiency of these mRNAs was compared to that of the corresponding molecules deleted from the UA-rich sequence [SP64GMAU$^-$ and soIF 3′*fos* AU$^-$ (Fig. 3)]. The removal of the UA-rich sequence from both mRNAs leads to a great increase of their translation efficiency (Fig. 4). These results suggest that all the mRNAs containing similar UA-rich sequences are submitted to the translational control we have identified.

The effect of UA-rich sequences on translation was not caused by rapid degradation of the mRNA. In fact, the IFN-β transcripts (Fig. 1) containing various numbers of copies of the UA-rich octanucleotide remained stable in the oocyte at least for the time of the translation assay (*15*). The same results were obtained with the GM-CSF mRNA. As determined by Northern blots (Fig. 4B), the GM-CSF mRNA either with or without the UA-rich sequence was not significantly degraded after 24 hours. These observations could reflect the absence in oocytes of somatic cell factor, or factors, responsible for rapid degradation of mRNAs containing UA-rich sequences. Wilson *et al.* (*16*) have shown that the removal of the poly(A) and subsequent degradation of c-*fos* mRNA are facilitated in somatic cells by the UA-rich sequences, and that ongoing translation of the mRNA seems to be required for this degradation process to occur. Since the translation of the UA-rich mRNAs are inhibited in frog oocytes, a rapid degradation of these messengers would not be expected if the mechanism described by Wilson *et al.* is operating. Moreover, poly(A) shortening is very limited in frog oocytes (*17*). This may also account for the high stability of the GM-CSF mRNA even with the UA-rich sequence.

So far, no *Xenopus* oocyte mRNA containing 3′ UA-rich sequences has been identified. However, during oogenesis, many maternal mRNAs are accumulated as untranslated messenger ribonucleoproteins (mRNPs) and are loaded into polysomes only after activation or fertilization of the oocyte (*18*). The mechanisms of these translational controls are still not elucidated. Although the maternal mRNAs characterized until now don't have 3′ UA-rich sequences, it does not exclude however that the translation inhibition mediated by these sequences could be one regulation by which the oocyte modulates the expression of some maternal mRNAs.

Is the translational control by the UA-rich sequence also exerted in somatic cells? Translational regulation of UA-containing mRNAs in somatic cells may be masked by the rapid turnover of those mRNAs. The mRNAs of mouse tumor necrosis factor (TNF) (*19*), c-*fos* (*20*), or IFN (*21*) could be the targets of a translational control mechanism coupled with a ribonucleolytic regulation. Recently, Beutler *et al.* (*22*) have suggested that the principal cause of instability conferred by UA-rich sequences is their content of UpA dinucleotide. Since the translational regulation seems to require a longer and more complex UA motif, the UA-rich sequence may have been retained largely to effect the translational control. In the *Xenopus* oocyte, the mRNAs with high content of UpA dinucleotide are not rapidly degraded. This system may be useful, therefore, for examining the mechanism through which UA-rich sequences mediate their negative translational control.

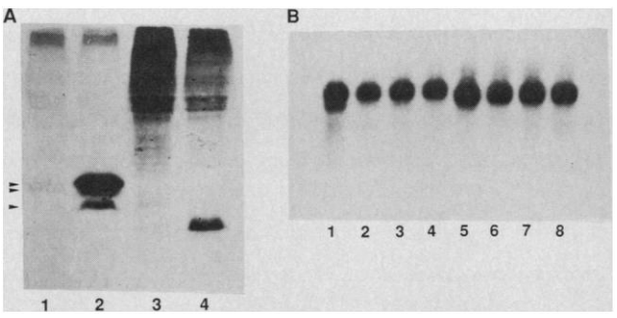

Fig. 4. (**A**) Translation in *Xenopus* oocytes of the GM-CSF and the chimeric IFN-β–c-*fos* mRNAs deleted or not from the UA-rich sequence in oocytes. The RNAs were synthesized by in vitro transcription of the plasmids described in Fig. 3, previously linearized by Hind III (for psoIF 3′*fos* and psoIF 3′*fos* AU$^-$) or by Bgl II for pSP64GM and pSP64GMAU$^-$. The translation procedure is the same as described in legend to Fig. 2 except that sheep polyclonal antibody to human GM-CSF was used to analyze the GM-CSF mRNAs translation. In order to ensure that the transcripts were not altered by the cloning procedure, their translation efficiency was also checked in the wheat germ extract (*26*). In that system, the mRNAs were translated with the same efficiency independently from the presence or not of UA-rich sequences. Lane 1, soIF 3′*fos*; lane 2, soIF 3′*fos* AU$^-$; lane 3, SP64GM; and lane 4, SP64GMAU$^-$. (**B**) Stability of the SP64GM and SP64GMAU$^-$ mRNAs in *Xenopus* oocytes. In vitro transcribed RNA was injected at 2 ng per oocyte. Total RNA was extracted from a batch of ten oocytes after specified incubation times (*17*) and 8 μg of total RNA were denatured by a glyoxal dimethylsulfoxide treatment and separated on a 1.4% agarose gel before Northern blot analysis. The GM-CSF mRNA was revealed by hybridization of the filter with a DNA probe corresponding to the coding and 3′ noncoding regions of the GM-CSF gene (*25*). Lanes 1 to 4 correspond to the complete GM-CSF mRNA remaining in oocytes after 0, 6, 12, and 24 hours, respectively. Lanes 5 to 8 correspond to the deleted GM-CSF mRNA remaining in oocytes after the same incubation times.

REFERENCES AND NOTES

1. D. R. Drummond *et al.*, *Nucleic Acids Res.* **13**, 7375 (1985).
2. M. Kozak, *Cell* **44**, 283 (1986).
3. J. Pelletier and N. Sonenberg, *ibid.* **40**, 515 (1985).
4. M. Kozak, *Microbiol. Rev.* **47**, 1 (1983).
5. G. Huez *et al.*, *Eur. J. Biochem.* **130**, 205 (1983).
6. M. F. Grossi de Sa *et al.*, *ibid.* **176**, 521 (1988).
7. M. W. Hentze *et al.*, *Proc. Natl. Acad. Sci. U.S.A.* **84**, 6730 (1987).
8. S. Strickland *et al.*, *Science* **241**, 680 (1988).
9. V. Kruys *et al.*, *Proc. Natl. Acad. Sci. U.S.A.* **84**, 6030 (1987).
10. N. B. K. Raj and P. M. Pitha, *ibid.* **78**, 7426 (1981).
11. V. Kruys, M. Wathelet, G. Huez, *Gene* **72**, 191 (1988).
12. D. Caput *et al.*, *Proc. Natl. Acad. Sci. U.S.A.* **83**, 1670 (1986).
13. G. Shaw and R. Kamen, *Cell* **46**, 659 (1986).
14. V. Kruys *et al.*, unpublished gel retardation experiments.
15. V. Kruys *et al.*, unpublished RNA blot analysis.
16. T. Wilson and R. Treisman, *Nature* **336**, 396 (1988).
17. G. Marbaix *et al.*, *Proc. Natl. Acad. Sci. U.S.A.* **72**, 3065 (1975).
18. E. H. Davidson, *Gene Activity in Early Development* (Academic Press, New York, ed. 2, 1976).
19. B. Beutler *et al.*, *Science* **232**, 977 (1986).
20. R. L. Mitchell *et al.*, *Cell* **40**, 209 (1985).
21. J. Shuttleworth *et al.*, *J. Gen. Vir.* **58**, 25 (1982).
22. E. Beutler *et al.*, *Proc. Natl. Acad. Sci. U.S.A.* **86**, 192 (1989).
23. F. Meijlink *et al.*, *ibid.* **82**, 4987 (1985).
24. J. Deschamps and I. Verma, unpublished data.

25. G. G. Wong *et al.*, *Science* **228**, 810 (1985).
26. V. Kruys *et al.*, unpublished data.
27. We are grateful to E. Declercq and A. Billiau for providing us the goat anti-human IBN-β antiserum and to the Glaxo Institute (Geneva) for sending us anti-human GM-CSF antiserum. This work was supported by ULB–Actions de Recherches Concertées of the Belgian Government and Crédit aux Chercheurs from the Belgian National Fund for Scientific Research to G.H. O.M. is supported by a grant from the Institute for Encouragement of Scientific Research in Industry and Agriculture.

17 February 1989; accepted 23 May 1989

Osteoclastic Bone Resorption by a Polarized Vacuolar Proton Pump

HARRY C. BLAIR, STEVEN L. TEITELBAUM, ROBERT GHISELLI, STEPHEN GLUCK*

Bone resorption depends on the formation, by osteoclasts, of an acidic extracellular compartment wherein matrix is degraded. The mechanism by which osteoclasts transport protons into that resorptive microenvironment was identified by means of adenosine triphosphate–dependent weak base accumulation in isolated osteoclast membrane vesicles, which exhibited substrate and inhibition properties characteristic of the vacuolar, electrogenic H^+-transporting adenosine triphosphatase (H^+-ATPase). Identity of the proton pump was confirmed by immunoblot of osteoclast membrane proteins probed with antibody to vacuolar H^+-ATPase isolated from bovine kidney. The osteoclast's H^+-ATPase was immunocytochemically localized to the cell-bone attachment site. Immunoelectron microscopy showed that the H^+-ATPase was present in the ruffled membrane, the resorptive organ of the cell.

THE OSTEOCLAST, WHICH IS THE principal resorptive cell of the skeleton, degrades both the inorganic and organic components of bone in a localized area at its matrix attachment site. Although the complete mechanism by which the cell resorbs bone is unknown, it is believed to involve acidification of the osteoclast-bone interface (*1–3*). This hypothesis rests on the fact that bone mineral is hydroxyapatite, $Ca_3(PO_4)_2Ca(OH)_2$, an alkaline salt, and hence its dissolution requires protonation, ~2 moles of H^+ for each mole of Ca^{2+} placed into solution.

Baron *et al.* (*4*) reported that the cell's characteristic resorptive organ, the ruffled membrane, expresses on its extracellular domain a 100-kD protein that reacts with antibody to the vanadate-sensitive hydrogen and potassium-dependent adenosine triphosphatase (H^+,K^+-ATPase) of gastric parietal cells. We undertook experiments aimed at assessing the function of the osteoclast's H^+ transport system by exploiting the property of weak bases of low molecular mass to diffuse into acidic compartments where they are trapped by protonation, raising the *p*H (*5*). Starting with highly enriched (95% to 98% pure) populations of osteoclasts isolated from calcium-deprived laying hens (*6*), we produced membrane vesicles by differential centrifugation after homogenization of osteoclasts in isotonic sucrose buffer (*7*) and used acridine orange, a fluorescent weak base *p*H indicator, to determine proton transport in response to exogenous nucleoside triphosphate addition in the presence and absence of specific inhibitors (*7, 8*). We found that osteoclast membranes were capable of adenosine triphosphate (ATP)–dependent H^+ transport (Fig. 1). Vesicle acidification was not inhibited by 1 m*M* sodium orthovanadate, an agent that completely damps the gastric H^+,K^+- and other E_1E_2-type ATPases (*9*). The osteoclast's proton pump was also resistant to the mitochondrial H^+-ATPase inhibitor oligo-

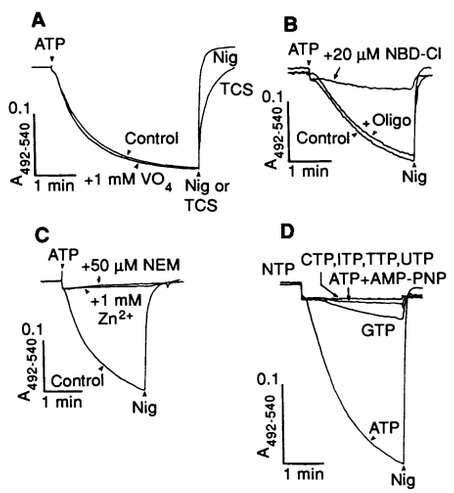

Fig. 1. ATP-dependent proton transport by isolated inside-out osteoclast membrane vesicles. Proton transport was assayed with a dual-wavelength spectrophotometer by monitoring uptake of acridine orange, as described (*6*), with 25 μg of membrane vesicles in 1 ml of buffer containing 150 m*M* KCl, 10 m*M* bis-tris-propane, 2 m*M* $MgCl_2$, and 1 μ*M* valinomycin, *p*H 7.0, and was initiated by the addition of 1 m*M* ATP (or other nucleotides, as described). The protonophores nigericin (Nig), 1 μm, or tetraclorosalicylanilide (TCS), 1 μm, were added as indicated. (**A**) Control, and with addition of 1 m*M* sodium orthovanadate; (**B**) control, with addition of oligomycin (5 μg/ml), and with addition of 20 μ*M* 7-chloro-4-nitrobenz-2-oxa-1,3-diazole (NBD-Cl); (**C**) control, with addition of 50 μ*M* *N*-ethylamleimide (NEM), and with addition of 1 m*M* $ZnCl_2$; and (**D**) 1 m*M* of each nucleotide [1 m*M* 5′-adenylylimide-diphosphate (AMP-PNP) was added prior to ATP addition]. Vesicles were prepared from 2×10^7 osteoclasts, obtained as described (*6*), homogenized in a Dounce homogenizer (20 strokes) in 15 ml of 250 m*M* sucrose, 5 m*M* tris, 1 m*M* EGTA, 1 m*M* $KHCO_3$, and 1 m*M* dithiothreitol, *p*H 7.0, at 4°C. After an initial centrifugation (1000*g* for 5 min), the supernatant was centrifuged (6000*g* for 15 min) to remove mitochondria and lysosomes. The supernatant was centrifuged at 42,000*g* for 30 min, and the upper, white microsomal layer of the pellet was collected. $A_{492\text{-}540}$, differences in absorbance at 492 nm and 540 nm.

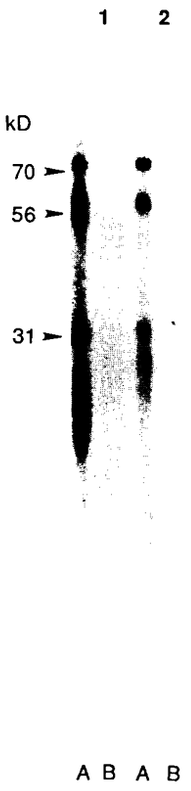

Fig. 2. Immunoblot of osteoclast microsomal proteins or purified bovine kidney H^+-ATPase probed with (lanes A) antiserum to H^+-ATPase or (lanes B) preimmune serum. Immunoreactivity of 70-, 56-, and 31-kD subunits seen in the kidney H^+-ATPase are also present in the osteoclast membranes. (Sample 1) Affinity-purified bovine kidney H^+-ATPase (5 μg) (*9*) and (sample 2) osteoclast microsomes (50 μg) were separated by SDS–polyacrylamide gel electrophoresis, transferred to nitrocellulose paper, and probed with antiserum or control serum as described (*9*); ^{125}I-labeled protein A and autoradiography were used for detection.

H. C. Blair and R. Ghiselli, Department of Pathology, Jewish Hospital at Washington University Medical Center, St. Louis, MO 63110.
S. L. Teitelbaum, Department of Pathology, Jewish Hospital at Washington University Medical Center, St. Louis, MO 63110, and Shriners' Hospital for Crippled Children, St. Louis, MO 63130.
S. Gluck, Renal Division, Department of Medicine, Jewish Hospital at Washington University Medical Center, St. Louis, MO 63110.

*To whom correspondence and requests for reprints should be addressed.